Electronic Supplementary Material (ESI) for Journal of Materials Chemistry C.

Efficient blue fluorescent OLEDs based on a D-π-A emitter with the hybridized local and charge transfer excited state

Xin Xia, Wenjuan Cao, Ming Zhang, Feng Li*

State Key Laboratory of Supramolecular Structure and Materials, College of Chemistry, Jilin University, Qianjin Avenue 2699, Changchun, 130012, P. R. China

*E-mail: lifeng01@jlu.edu.cn

Contents

General information

All reagents and solvents required for synthesis and characterization are purchased from commercial suppliers and used directly without any treatment. A

Bruker AvanceIII 500 NMR spectrometer was used for the 1H data collection in CDCl3 solvent with tetramethylsilane as the internal standard. Mass spectra of all compounds were recorded on Thermo Fisher ITQ1100 GC-MS mass detector. A shimadzu UV-2550 spectrophotometer was applied to record the ultraviolet (UV)-visible spectra. Fluorescence spectra were recorded using a RF-5301 PC spectrophotometer. The electrochemical oxidation and reduction potentials were recorded using an electrochemical analyzer (CHI660C, CH Instruments, USA). The fluorescence decay spectra were recorded on an Edinburgh fluorescence spectrometer (FLS980), and the lifetime of the excited states was measured by the time-correlated single photon counting method under the excitation of a laser (375 nm) with a pulse width of 50 ps. Thermal gravimetric analysis (TGA) were characterized by a TA INSTRUMENTS Q500 TGA analyzer. Differential scanning calorimetry (DSC) was measured on a Netzsch DSC204 instrument at a heating rate of 10℃ min^{-1} from 20℃ to 400℃ under nitrogen flushing.

Device fabrication and measurement

Ready-made indium tin oxide (ITO) glass substrates were purchased and cleaned with ethanol, acetone, toluene and isopropyl alcohol. After dried with N_2, they were treated with UV irradiation for 20 min and transferred to a vacuum deposition system with the pressure of $4–6\times10^{-6}$ mbar. The MoO_3 layer was deposited at a rate of 0.2 Å s^{-1}. All the organic layers were deposited at 0.3–0.5 Å s^{-1}. The evaporation rate of cathode LiF and Al metal layer were 0.1 Å s^{-1} and 0.6–1.2 Å s^{-1} respectively. The current-voltage-bright (I-V-B) characteristics were measured using a Keithley 2400

programmable electrometer combined with a Photo Research spectroradiometer (PR-650). The EL spectra and CIE coordination were measured using a Photo Research spectroradiometer (PR-650) at room temperature under ambient conditions.

1. Synthesis

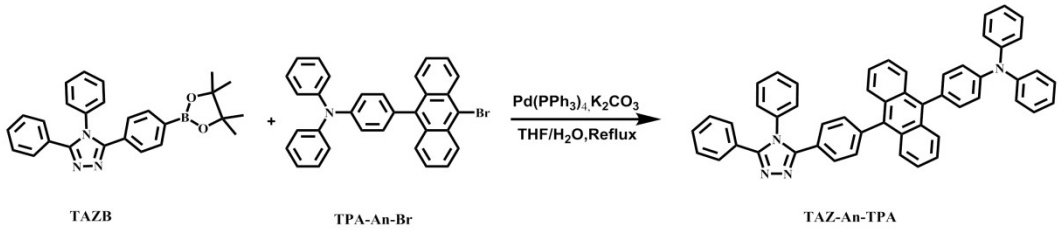

Scheme 1. Synthetic routes and chemical structures of TAZ-An-TPA

The compounds TAZB and TPA-An-Br were synthesized according to our previous report. TAZB (0.5 g, 1.18 mmol), TPA-An-Br (0.7 g, 1.42 mmol) were added into a clean double-mouth flask and dissolved with 30 mL ultra-dry THF at first. Then, K_2CO_3 (1.8 g, 13 mmol) was dissolved in 16mL of deionized water and transferred the aqueous solution of metal salt into the flask with a syringe. After stirring, (0.068 g, 0.059 mmol) $Pd(PPh_3)_4$ catalyst was added to the reaction flask, frozen with liquid nitrogen and then thawed under vacuum until the reaction system was near room temperature. Then the mixture was stirred at 70 °C for 36 h in a closed system under the protection of nitrogen. After the reaction was completed and cooled, the mixture was extracted with dichloromethane and water several times, and the organic phase was dried over anhydrous $MgSO_4$. The residue was purified via column

chromatography by using the dichloromethane/ethyl acetate (3 : 1, v/v) mixture as the eluent. A white power was obtained. (0.55 g, yield: 66%). The product was further sublimated to obtain higher-purity sublimates.^{1}H NMR (500 MHz, CD_2Cl_2) δ 7.88 (d, J = 8.5 Hz, 2H), 7.74 (d, J = 8.0 Hz, 2H), 7.65 (d, J = 8.5 Hz, 2H), 7.57 (dd, J = 15.6, 7.2 Hz, 5H), 7.49 (t, J = 10.5 Hz, 3H), 7.46 – 7.26 (m, 20H), 7.13 (t, J = 7.3 Hz, 2H). MS(m/z) calculated for $C_{52}H_{36}BrN_4$：716.89; Found, 718.80.

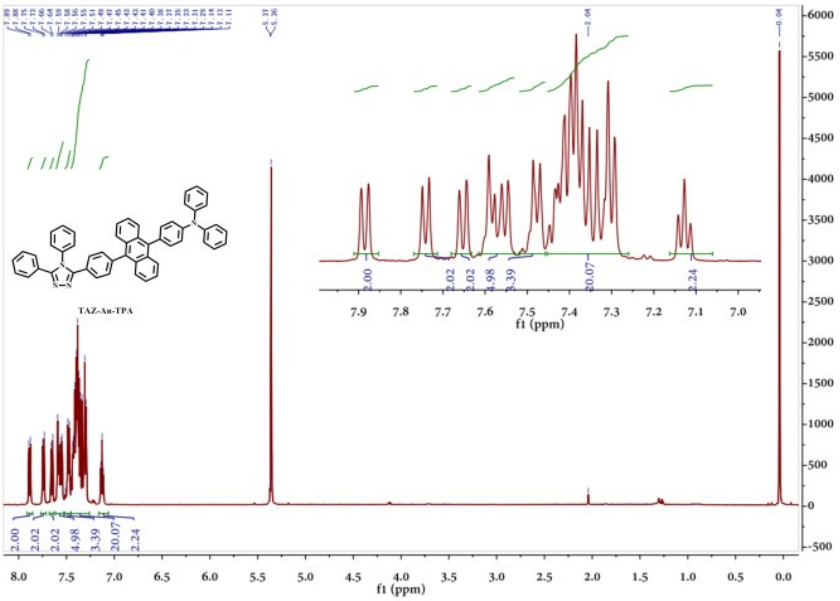

Figure S1. ^{1}H NMR spectrum of TAZ-An-TPA in CD_2Cl_2.

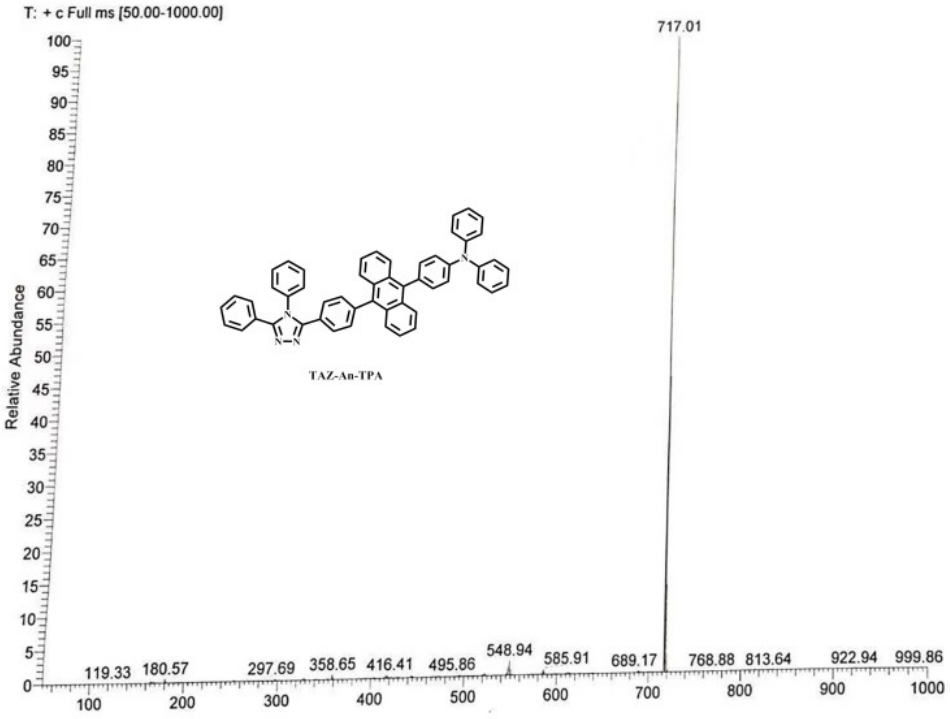

Figure S2. Mass Spectrum of TAZ-An-TPA.

2. Thermal and Electrochemical Properties

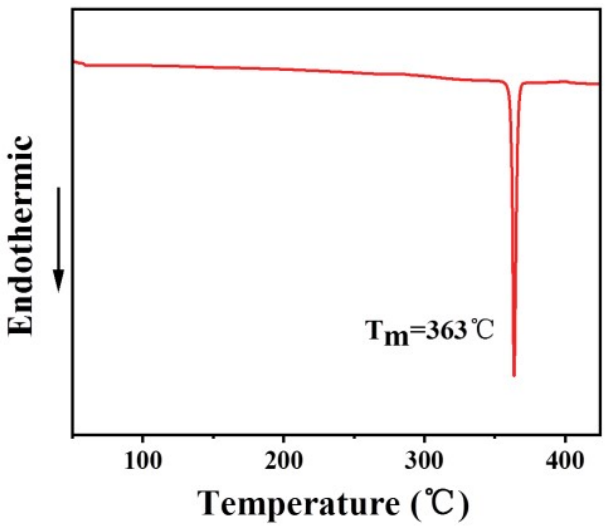

Figure S3. Diffefential scanning calorimetry (DSC) curves of TAZ-An-TPA.

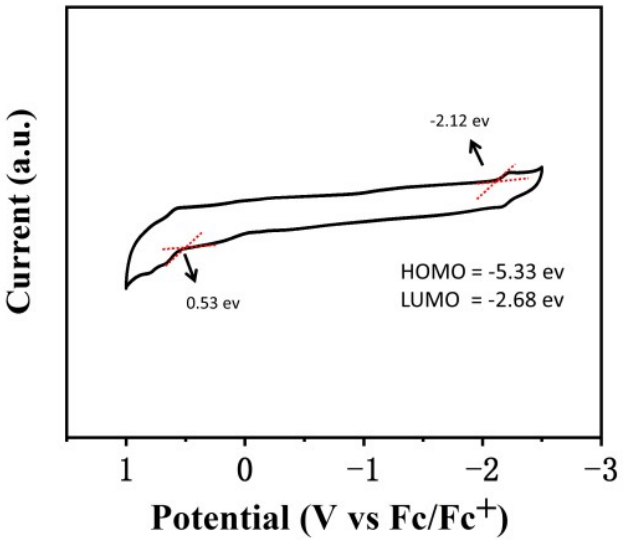

Figure S4. Cyclic voltammogram curve of TAZ-An-TPA in DMF.

3. Photophysical Properties

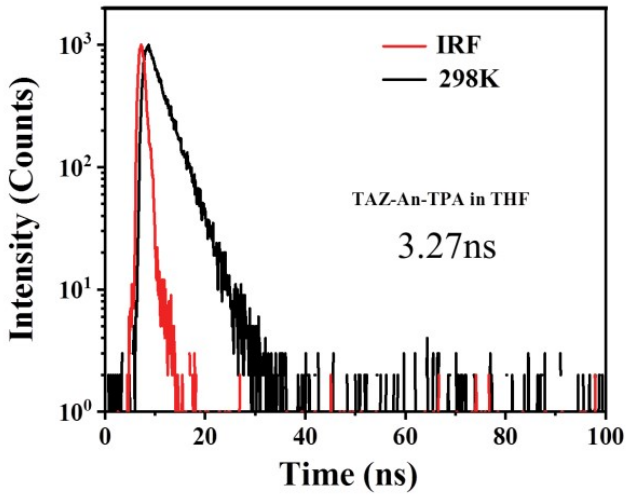

Figure S5. The transient PL decay of the TAZ-An-TPA in THF (at room temperature；λ_{ex}=375nm，λ_{em}=483nm).

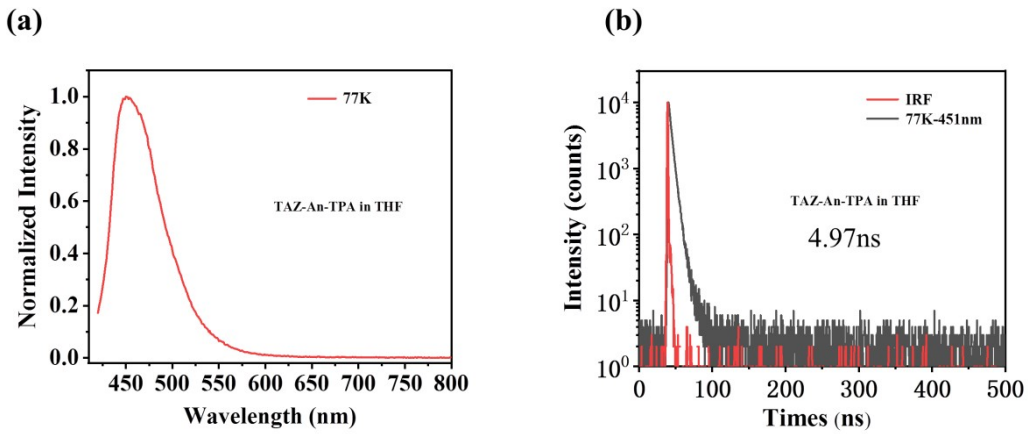

Figure S6. a) PL spectra of TAZ-An-TPA in THF (at 77K); b) The transient PL decay of the TAZ-An-TPA in THF (at 77K; λ_{ex}=375nm, λ_{em}=451nm).

Table S1. Photophysical properties of TAZ-An-TPA in different solvents.

Solvents	Δ_f	ν_a (nm)[a]	ν_f (nm) [b]	ν_a-ν_f (cm^{-1}) [c]	PLQY (%) [d]
Hexane	0	403	444	2291	43.3
Toluene	0.013	405	456	2884	44.8
Tetrahydrofuran	0.209	403	476	3727	50.1
Dichloromethane	0.217	403	491	4447	55.9
Acetonitrile	0.305	405	506	4889	36.3

[a]UV peaks in different solvents at room temperature. [b] PL peaks in different solvents at room temperature. [c]Stokes shift in different solvents [d] PLQY in different solvents at room temperature.

4. Theoretical Calculations

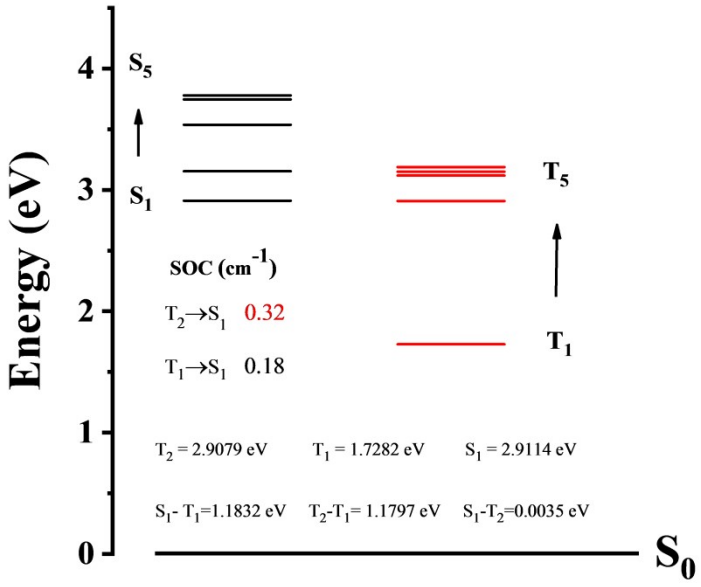

Figure S7. Calculated energy levels of the first five singlet/triplet states and the SOC matrix element values of TAZ-An-TPA.

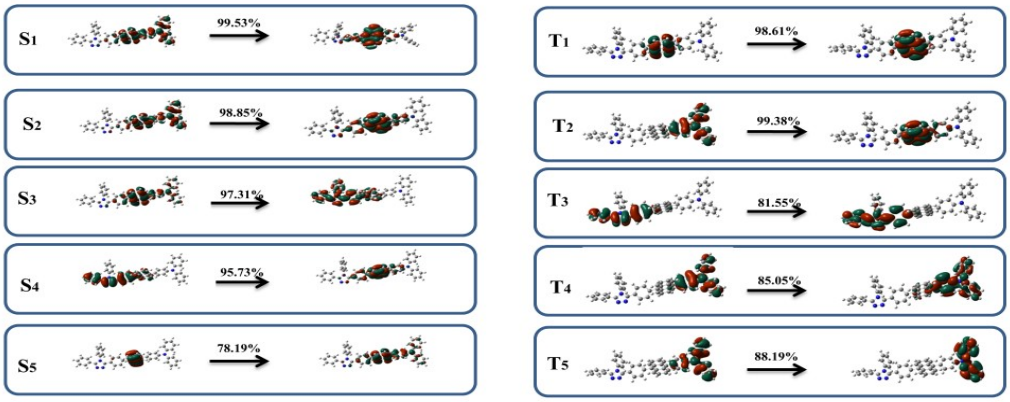

Figure S8. The NTO transition character of the first five singlet and triplet states

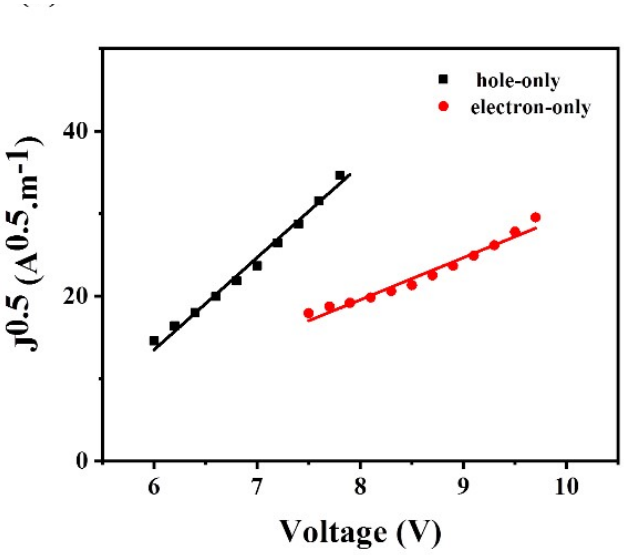

Figure S9. The carrier mobility calculated from the $J^{1/2}$ - V curves of the single-carrier devices according to the SCLC model.

5. Electroluminescence Performances

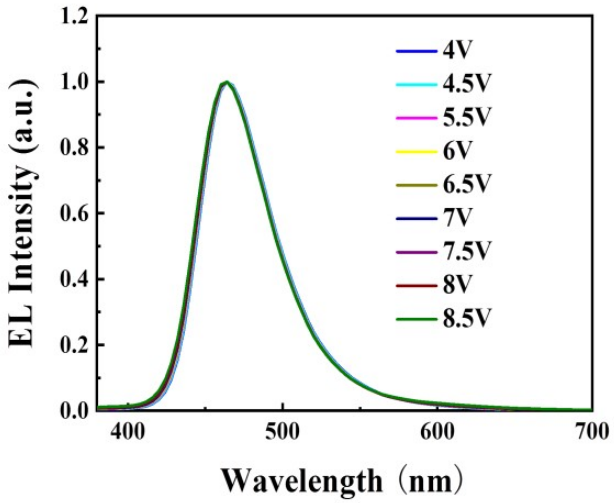

Figure S10. The EL spectra of based TAZ-An-TPA OLEDs at different voltages.

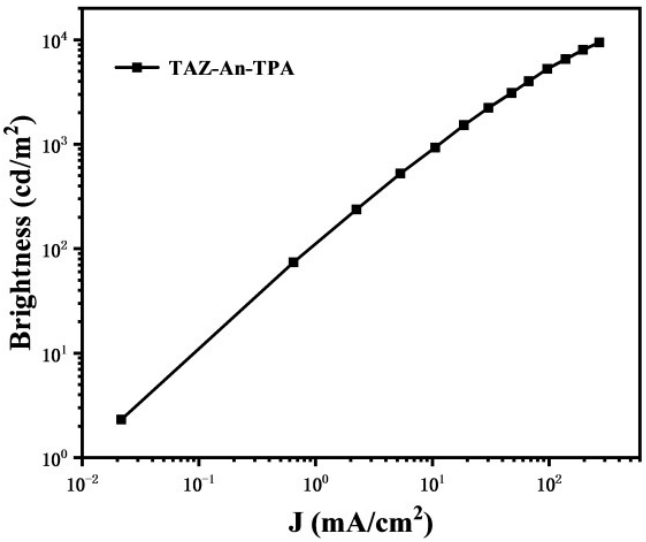

Figure S11. Luminance-current density characteristics of TAZ-An-TPA OLED

6. Device performance of TAZ-An-TPA OLEDs with other structures

Device I: ITO/MoO3 (3nm)/TAPC (40nm)/TAZ-An-TPA (20nm)/TPBi (40nm)/LiF (1nm)/Al (100nm)

Device II: ITO/MoO3 (3nm)/TAPC (25nm)/TCTA (15nm)/TAZ-An-TPA (20nm)/TPBi (40nm)/LiF(1nm)/Al (100nm)

Device III: ITO/MoO3 (3nm)/TAPC (40nm)/CBP: TAZ-An-TPA (10.0% wt, 20nm)/TPBi (40nm)/LiF (1nm)/Al (100nm)

Table S2. Performance of the Devices I, II, and III.

Emitter	V_{on} (V) [a]	L_{max} (cd m^{-2})	CE (cd A^{-1}) [b]	PE (lm W^{-1}) [c]	EQE (%) [d]	λ_{EL} (nm)	CIE (x, y)
Device I	3.0	16710	11.7	8.3	6.7	476	(0.151,0.257)
Device II	3.0	11750	9.6	7.2	5.0	476	(0. 185,0.288)
Device III	3.5	10970	10.1	9.0	7.5	464	(0.148, 0.165)

[a] Turn-on voltage at 1 cd m^{-2}. [b] Maximum current efficiency. [c]Maximum power efficiency. [d]Maximum EQE.

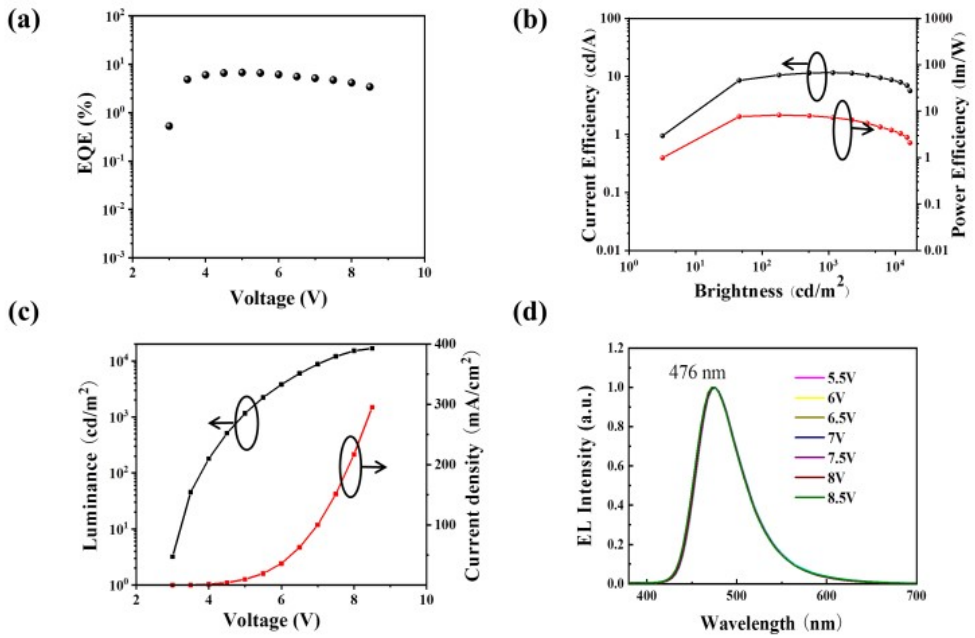

Figure S12. Performance of Device I. a) The external quantum efficiency versus current density; b) EL spectrum of the OLEDs; c) The J-V-L characteristics of the OLEDs; d) The external quantum efficiency versus current density.

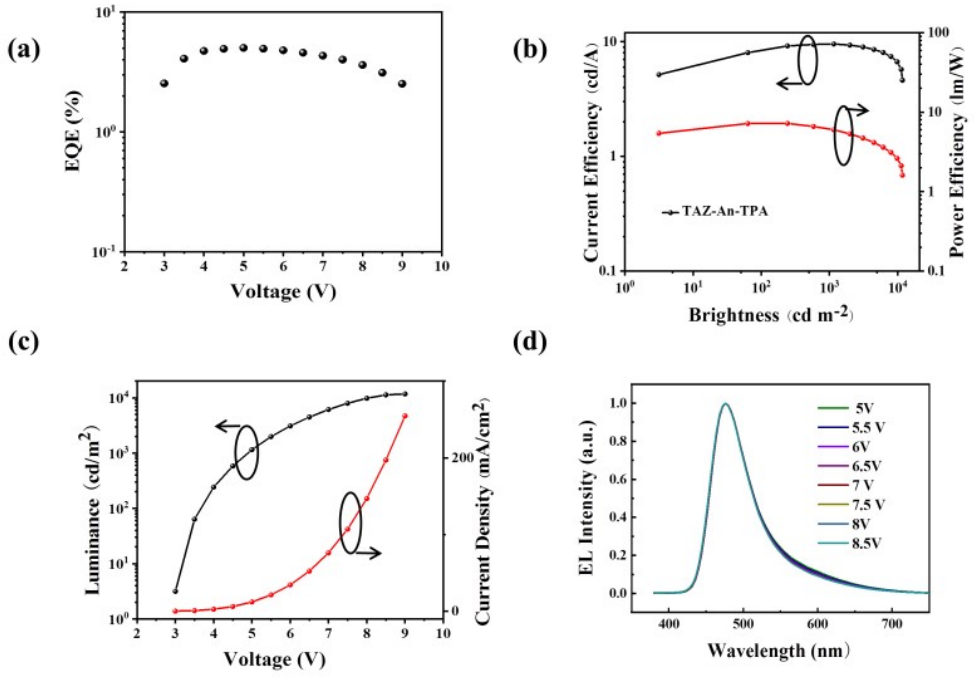

Figure S13. Performance of Device II. a) The external quantum efficiency versus current density; b) EL spectrum of the OLEDs; c) The J-V-L characteristics of the OLEDs; d) The external quantum efficiency versus current density.

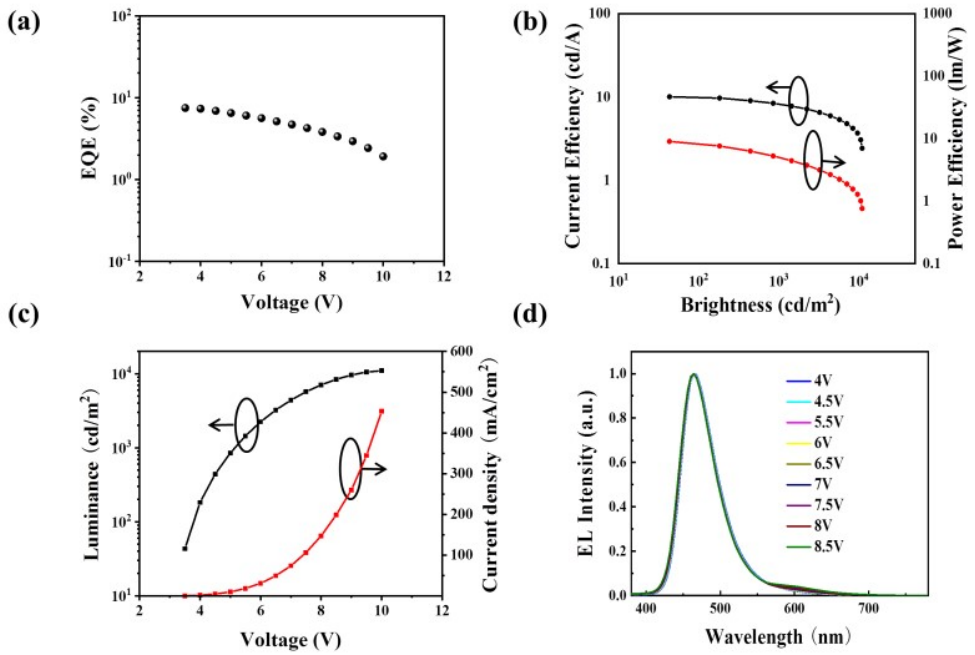

Figure S14. Performance of Device III. a) The external quantum efficiency versus current density; b) EL spectrum of the OLEDs; c) The J-V-L characteristics of the OLEDs; d) The external quantum efficiency versus current density.

7. References

1. W. Cao, A. Abdurahman, P. Zheng, M. Zhang and F. Li, *Journal of Materials Chemistry C*, 2021, **9**, 6873-6879.
2. A. Abdurahman, A. Obolda, Q. Peng and F. Li, *Dyes and Pigments*, 2018, **153**, 10-17.
3. S. Zeng, C. Xiao, J. Zhou, Q. Dong, Q. Li, J. Lim, H. Ma, J. Y. Lee, W. Zhu and Y. Wang, *Advanced Functional Materials*, 2022, **32**.
4. J. Jayabharathi, J. Anudeebhana, V. Thanikachalam and S. Sivaraj, *Journal of Materials Chemistry C*, 2021, **9**, 15683-15697.
5. J. M. Ha, S. H. Hur, A. Pathak, J.-E. Jeong and H. Y. Woo, *Npg Asia Materials*, 2021, **13**.
6. Y. Xu, X. Liang, X. Zhou, P. Yuan, J. Zhou, C. Wang, B. Li, D. Hu, X. Qiao, X. Jiang, L. Liu, S. J. Su, D. Ma and Y. Ma, *Advanced materials*, 2019, **31**, e1807388.
7. S. Zhang, L. Yao, Q. Peng, W. Li, Y. Pan, R. Xiao, Y. Gao, C. Gu, Z. Wang, P. Lu, F. Li, S. Su, B. Yang and Y. Ma, *Advanced Functional Materials*, 2015, **25**, 1755-1762.
8. X. L. Yang, X. B. Xu and G. J. Zhou, *Journal of Materials Chemistry C*, 2015, **3**, 913-944.

9. F. Liu, X. Man, H. Liu, J. Min, S. Zhao, W. Min, L. Gao, H. Jin and P. Lu, *Journal of Materials Chemistry C*, 2019, **7**, 14881-14888.
10. C. Zhou, D. Cong, Y. Gao, H. Liu, J. Li, S. Zhang, Q. Su, Q. Wu and B. Yang, *The Journal of Physical Chemistry C*, 2018, **122**, 18376-18382.
11. J. D. Girase, Shahnawaz, J.-H. Jou, S. Patel and S. Vaidyanathan, *Dyes and Pigments*, 2022, **206**.
12. J. Shi, Q. Ding, L. Xu, X. Lv, Z. Liu, Q. Sun, Y. Pan, S. Xue and W. Yang, *Journal of Materials Chemistry C*, 2018, **6**, 11063-11070.
13. W. Li, Y. Pan, R. Xiao, Q. Peng, S. Zhang, D. Ma, F. Li, F. Shen, Y. Wang, B. Yang and Y. Ma, *Advanced Functional Materials*, 2014, **24**, 1609-1614.
14. Y. Xu, P. Xu, D. Hu and Y. Ma, *Chemical Society reviews*, 2020, DOI: 10.1039/d0cs00391c.